

Response to Comments by Referee #1

Thank you for your commendation and appreciate your suggestions on all scientific, technical aspects of our article. The manuscript has been revised accordingly. Listed below is our point-to-point response to each comment.

General comments:

This paper reports a comparison of primary emissions and secondary organic aerosol formation from one gasoline direct injection (GDI) and one port fuel injection (PFI) gasoline vehicle. There is a limited but nonetheless useful study and interpretation of the formation of secondary organic aerosol (SOA) in relation to the low molecular weight aromatic compounds contained within the exhaust. My main concern over this paper is that previous work has shown quite substantial variations between vehicles of similar engine specification using the same fuel, and hence comparing one GDI vehicle with one PFI vehicle and then making very general statements about one technology versus another has the potential to mislead seriously. In this context, the title of the paper is most inappropriate as there is no evidence that the vehicles tested are representative of GDI and PFI vehicles more generally. For this reason, major modifications are recommended and the overall tenor of the paper needs to be much more subdued in relation to the comparison.

Response: We thank the referee for pointing out this. The gasoline vehicles tested in this study are representative in market share in China. And we agree with the referee that one vehicle for each gasoline engine technology exists uncertainty. We will conduct more experiments with more vehicles. We have revised title and added discussions as the suggestion.

The title is revised as: "Comparison of primary aerosol emission and secondary aerosol formation from gasoline direct injection and port fuel injection vehicles".

Following discussions are added between Line 312 to Line 315: "It should be pointed out that the SOA formation factors in this study are based on one GDI vehicle and one PFI vehicle. Some previous studies proposed that vehicles have variations even though they meet similar specification vehicles and use the same fuel (Gordon et al., 2014; Jathar et al., 2014). Thus more researches with more vehicles for each technology are needed on SOA formation from vehicle exhaust".

There are also issues over the way in which the technologies are described. Lines 25-26 state that "these studies show that GDI vehicles emit more primary particles than PFI vehicles, and even diesel vehicles equipped with diesel particulate filter" and lines 289-290 state that "the considerable particle number emitted by gasoline vehicles, especially in GDI vehicles exhaust... needs to be controlled in the future emissions standards". This ignores the fact that the European Euro 6 regulations set a particle mass and a number emissions standard for GDI which is the same as the emissions standard for diesel vehicles and consequently GDI engines with high particle emissions are fitted with particulate filters in order to meet the emissions regulations. Such filters will remove elemental carbon and POA as well as reducing the emission of organic vapors (as they have catalytic

activity), and consequently SOA production will be substantially reduced. Thus, the GDI vehicle tested in this study is almost certainly not representative of current GDI vehicles on sale in Europe (and most probably North America, although I am less familiar with that market) and for this reason also, the presentation of the results is likely to prove highly misleading.

Response: Thanks for the suggestion. In China, the PN will be restricted in China Phase VI Emissions Standard in 2020, so the gasoline particulate filters (GPFs) have not been used widely. The gasoline vehicles certified China Phase IV and V Emissions Standard dominate current on-road gasoline vehicles. Thus, this study could reflect the gasoline vehicle emissions in China and other developing countries. Moreover, it should be acknowledged that the GPFs have significant contribution on reducing primary aerosol emission from GDI vehicles (Chan et al., 2014). Some studies also reported that the VOCs emission from GDI vehicles might be reduced by catalyzed GPFs (Ito et al., 2015), which would lead to SOA formation reduction. Therefore, further studies on GPFs are needed in our future studies.

Specific comments:

Other points worthy of attention are the following: (a) Line 71 states that the gasoline fuel meets the China phase V fuel standard. This means nothing to the general reader. Fuel quality standards have in recent years been driven by sulphur content. As a minimum, the sulphur content of this fuel should be indicated.

Response: Thanks for your suggestion. Accepted, and adding sulfur content of the fuel between Line 88 to Line 90: “The fuel used in the experiments was a typical Phase V gasoline on the China market (sulfur content = 6 mg kg⁻¹). More information of the fuel is provided in Table S1 in the Supplement”.

Table S1 Details of the fuel used in the experiments.

Specifications	Fuel
Density (g mL ⁻¹)	0.7
Rvp (kPa)	55.4
Aromatics (% v/v)	36.7
Olefin (% v/v)	15.4
Ethanol (% v/v)	0.01
Oxygen (% m/m)	0.02
Mn (mg kg ⁻¹)	< 0.1
Sulfur (mg kg ⁻¹)	6
T10 (°C)	55.4
T50 (°C)	109.9
T90 (°C)	164.3
Fbp (°C)	194.4

(b) Line 240-241 suggests that since semi-volatile vapours may partition more strongly into the particle phase at higher aerosol concentrations, this would increase SOA formation. There are two factors here. The authors appear to be referring to the partitioning of the oxidation products which will give an increase in SOA yield at higher pre-existing particle loadings. However, there is a second effect which may be more significant. If the precursors of the SOA partition more strongly into the condensed phase at higher ambient particle loadings, there will be less vapour phase compound present to be oxidised and therefore the rate of SOA production will be reduced. This point needs to be considered when discussing the SOA yields on page 9.

Response: Thanks for your suggestion. The two aspects are considered and added between Line 248 to Line 256:

“Although particle wall-loss correction as well as particle and gas dilution corrections were considered in this study, several factors may still contribute to the uncertainties of the SOA productions. First, the deposition of semi-volatile vapors to the chamber walls was not corrected, which may result in an underestimation of the rate of SOA production with a factor of 1.1-4.1 (Zhang et al., 2014). Second, under some ambient conditions such as severe urban haze events (Guo et al., 2014), particle mass concentrations can be as high as 200-300 $\mu\text{g m}^{-3}$, much higher than the $23 \pm 6 \mu\text{g m}^{-3}$ under the chamber condition in this study. High particle mass loadings are favorable for the partition of semi-volatile compounds into the particle phase, potentially increasing the rate of SOA production (Odum et al., 1996). Third, stronger partitioning of SOA precursors into the particle phase may reduce the oxidized products in the gas phase, which will potentially reduce the rate of SOA production (Seinfeld et al., 2003)”.

(c) Table 2 refers to measurement of OC/EC but does not specify the analyser or the protocol. This should be included.

Response: We thank the reviewer for reminding this. The instrument for OC/EC measurement is added between Line 126 to Line 128: “...to analyze the mass, organic carbon (OC) and elemental carbon (EC) emission factors using a balance and OC/EC analyzer (Sunset Lab, USA)”.

(d) Table 4 reports emission factors for PAH but does not specify which compounds.

Response: Thanks for the suggestions. The PAHs emission factor reported in this study is a sum of 31 polycyclic aromatic hydrocarbons compounds. Their emission factors are listed in the Table S2 in the Supplement.

Table S2 The EFs of Particulate-phase PAHs from GDI and PFI vehicles.

Compound	Emission factor (ng km ⁻¹)	
	GDI	PFI
Napthalene	0.025	<0.0001
1-Methylnaphthalene	<0.0001	<0.0001
2-Methylnaphthalene	0.012	0.004
2,6-Dimethylnaphthalene	0.006	0.003
Acenaphthylene	0.012	0.009
Acenaphthene	<0.0001	0.015
Fluorene	0.003	0.105
Methyl-fluorene	0.083	0.105
Dibenzofuran	0.006	0.039
Retene	0.009	0.011
9-Methylanthracene	<0.0001	0.013
Phenanthrene	0.244	0.069
Anthracene	0.048	0.018
Fluoranthene	0.201	0.034
Pyrene	0.246	0.029
Methyl-fluoranthene	0.004	0.007
Benzo[a]anthracene	0.006	0.036
Chrysene	0.020	0.065
Methyl-chrysene	<0.0001	0.007
Benzo[b]fluoranthene	0.034	0.147
Benzo[k]fluoranthene	0.041	0.129
Benzo[e]pyrene	0.028	0.051
Benzo[a]pyrene	0.012	0.041
Benzo[ghi]fluoranthene	0.095	0.027
Cyclopenta[cd]pyrene	<0.0001	0.032
Dibenzo[a,h]anthracene	<0.0001	<0.0001
Picene	<0.0001	<0.0001
Perylene	0.009	<0.0001
Benzo[ghi]perylene	<0.0001	<0.0001
Indeno[1,2,3-cd]pyrene	<0.0001	<0.0001
Coronene	<0.0001	<0.0001
Sum PAHs	1.144	0.994

Reference

- Chan, T. W., Meloche, E., Kubsh, J., and Brezny, R.: Black Carbon Emissions in Gasoline Exhaust and a Reduction Alternative with a Gasoline Particulate Filter, *Environmental science & technology*, 48, 6027-6034, 10.1021/es501791b, 2014.
- Guo, S., Hu, M., Zamora, M. L., Peng, J., Shang, D., Zheng, J., Du, Z., Wu, Z., Shao, M., Zeng, L., Molina, M. J., and Zhang, R.: Elucidating severe urban haze formation in China, *Proceedings of the National Academy of Sciences of the United States of America*, 111, 17373-17378, 10.1073/pnas.1419604111, 2014.
- Ito, Y., Shimoda, T., Aoki, T., Yuuki, K., Sakamoto, H., Kato, K., Their, D., Kattouah, P., Ohara, E. and Vogt, C.: Next Generation of Ceramic Wall Flow Gasoline Particulate Filter with Integrated Three Way Catalyst, *SAE Technical Paper 2015-01-1073*, 2015, doi:10.4271/2015-01-1073, 2015.
- Gordon, T. D., Presto, A. A., May, A. A., Nguyen, N. T., Lipsky, E. M., Donahue, N. M., Gutierrez, A., Zhang, M., Maddox, C., Rieger, P., Chattopadhyay, S., Maldonado, H., Maricq, M. M., and Robinson, A. L.: Secondary organic aerosol formation exceeds primary particulate matter emissions for light-duty gasoline vehicles, *Atmos. Chem. Phys.*, 14, 4661-4678, 10.5194/acp-14-4661-2014, 2014.
- Jathar, S. H., Gordon, T. D., Hennigan, C. J., Pye, H. O. T., Pouliot, G., Adams, P. J., Donahue, N. M., and Robinson, A. L.: Unspeciated organic emissions from combustion sources and their influence on the secondary organic aerosol budget in the United States, *Proc. Natl. Acad. Sci. USA*, 111, 10473-10478, 10.1073/pnas.1323740111, 2014.
- Odum, J. R., Hoffmann, T., Bowman, F., Collins, D., Flagan, R. C., and Seinfeld, J. H.: Gas/particle partitioning and secondary organic aerosol yields, *Environ. Sci. Technol.*, 30, 2580-2585, 10.1021/es950943+, 1996.
- Seinfeld, J. H., Kleindienst, T. E., Edney, E. O., and Cohen, J. B.: Aerosol growth in a steady-state, continuous flow chamber: Application to studies of secondary aerosol formation, *Aerosol Science and Technology*, 37, 728-734, 10.1080/02786820390214954, 2003.
- Zhang, X., Cappa, C. D., Jathar, S. H., McVay, R. C., Ensberg, J. J., Kleeman, M. J., and Seinfeld, J. H.: Influence of vapor wall loss in laboratory chambers on yields of secondary organic aerosol, *Proc. Natl. Acad. Sci. USA*, 111, 5802-5807, 10.1073/pnas.1404727111, 2014.

Comparison of primary aerosol emission and secondary aerosol formation from gasoline direct injection and port fuel injection vehicles

Zhuofei Du¹, Min Hu^{1,3*}, Jianfei Peng^{1†}, Wenbin Zhang², Jing Zheng¹, Fangting Gu¹, Yanhong Qin¹, Yudong Yang¹, Mengren Li¹, Yusheng Wu¹, Min Shao¹, Shijin Shuai²

1. State Key Joint Laboratory of Environmental Simulation and Pollution Control, College of Environmental Sciences and Engineering, Peking University, Beijing 100871, China

2. State Key Laboratory of Automotive Safety and Energy, Department of Automotive Engineering, Tsinghua University, Beijing 100084, China

3. Beijing Innovation Center for Engineering Sciences and Advanced Technology, Peking University, Beijing 100871, China

[†] Now at Department of Atmospheric Sciences, Texas A&M University, College Station, TX 77843, US

*Corresponding author: Min Hu, minhu@pku.edu.cn

Abstract

Gasoline vehicles greatly contribute to urban particulate matter (PM) pollution. Gasoline direct injection (GDI) engines, known as their higher fuel efficiency than that of port fuel injection (PFI) engines, have been increasingly employed in new gasoline vehicles. However, the impact of this trend on air quality is still poorly understood. Here, we investigated both primary emissions and secondary organic aerosol (SOA) formation from GDI and PFI vehicles under urban-like condition, using combined approaches involving chassis dynamometer measurement and environmental chamber simulation. The PFI vehicle emits slightly more volatile organic compounds, e.g., benzene and toluene, whereas the GDI vehicle emits more particulate components, e.g., the total PM, elemental carbon, primary organic aerosols and polycyclic aromatic hydrocarbons. Strikingly, a much higher SOA production (by a factor of approximately 2.7) is found from the exhaust of the GDI vehicle than that of the PFI vehicle under the

same conditions. More importantly, the higher SOA production found in the GDI vehicle exhaust occurs concurrently with lower concentrations of traditional SOA precursors, e.g., benzene and toluene, indicating a greater contribution of intermediate volatility organic compounds and semivolatile organic compounds in the GDI vehicle exhaust to the SOA formation. Our results highlight the considerable potential contribution of GDI vehicles to urban air pollution in the future.

1 Introduction

Organic aerosols account for approximately 20-50 % of ambient fine particulate matter (PM_{2.5}), with significant environment and health effects (Kanakidou et al., 2005). Primary organic aerosol (POA) is emitted directly by sources, while secondary organic aerosol (SOA) is mainly formed via oxidation of gaseous precursors in the atmosphere and account for about 30-90 % of the organic aerosol (OA) mass worldwide (Zhang et al., 2007; Hu et al., 2016), but SOA source remain poorly constrained. Robinson et al. (2007) proposed that low-volatility gas-phase species emitted from diesel vehicles were important sources for urban ambient SOA, which achieved better mass closure between observed and modeled SOA. Using an updated CMAQ model, Jathar et al. (2017) found that 30-40% OA was contributed from vehicles in the southern California, and half of which was SOA. Huang et al. (2014) recently revealed that 15-65 % of SOA was contributed by fossil fuel consumption (i.e., traffic and coal burning) in megacities in China. These indicated that vehicles have important contribution to ambient SOA in urban areas. An ambient organic aerosol measurement in the Los Angeles Basin demonstrated that SOA contributed from gasoline vehicles was significant in the urban air, much larger than that from diesel vehicles (Bahreini et al., 2012). Similar conclusion was reached by Hayes et al. (2013) based on mass spectrometer results. Meanwhile, several chamber simulation studies concluded that exhaust of gasoline vehicles could form substantial SOA (Jathar et al., 2014). Thus, gasoline vehicles exhaust is highly associated with ambient SOA formation.

Gasoline vehicles can be categorized into two types based on the fuel injection technologies in their engines, i.e., port fuel injection (PFI) vehicles and gasoline direct injection (GDI) vehicles. Unlike a PFI engine, in which

51 gasoline is injected into intake port, gasoline is sprayed into cylinder directly in a GDI engine. With the increased
52 atomization and vaporization rate of fuel, and more accurate control of fuel volume and injection time, a GDI
53 engine has many advantages, such as better fuel efficiency, lower CO₂ emissions and less fuel pumping loss
54 (Alkidas, 2007; Myung et al., 2012; Liang et al., 2013). In past decades, PFI vehicles dominated the market share
55 of gasoline cars in the world. However, in recent years, GDI vehicles have been increasingly employed, due to their
56 higher fuel efficiency. The market share of GDI vehicles in sales in 2016 reached about 25 %, 50 % and 60 % in
57 China, the US and Europe, respectively (Wen et al., 2016; Zimmerman et al., 2016).

58 Several previous studies investigated the emissions of GDI and PFI vehicles, in terms of concentrations of
59 gaseous pollutants, particle numbers and mass concentrations, and evaluated the reduction of emissions with the
60 upgrading emission standards (Ueberall et al., 2015; Zhu et al., 2016; Saliba et al., 2017). These studies show that
61 GDI vehicles emit more primary particles than PFI vehicles (Zhu et al., 2016; Saliba et al., 2017), and even diesel
62 vehicles equipped with diesel particulate filter (DPF) (Wang et al., 2016), which is likely due to insufficient time
63 allowed for gasoline fuel to be mixed with air thoroughly, as well as gasoline droplets impinging onto pistons and
64 surfaces of combustion chamber in GDI engine (Chen et al., 2017; Fu et al., 2017). However, in most studies,
65 vehicles were tested under the driving cycles of the US or European standards, indicating that those results are not
66 representative of China's traffic conditions.

67 SOA production from gasoline vehicle exhaust was previously simulated in smog chambers and potential
68 aerosol mass (PAM) flow reactors. SOA formed from gaseous pollutants exceeds the related POA emissions and
69 having much more contribution to air quality degradation. These studies mostly focused on the impacts of SOA
70 formation by the model year (Gordon et al., 2014; Jathar et al., 2014; Liu et al., 2015), fuel formulations (Peng et
71 al., 2017), driving cycles (including idling) (Nordin et al., 2013; Platt et al., 2013) and start-up modes of the gasoline
72 vehicles (Nordin et al., 2013). Few studies, however, have investigated SOA formation from vehicles with different
73 engine technologies (GDI and PFI) under the same working condition.

74 In this study, both primary emissions and secondary aerosol formation from GDI and PFI vehicles were
75 investigated. To represent typical urban driving patterns in megacities such as Beijing, the vehicles were tested

76 using gasoline fuel meeting the China Phase V fuel standard, and were operated with the cold-start Beijing cycle
77 (BJC). The SOA formation from both the PFI and GDI vehicle exhausts were then simulated using a smog chamber.
78 Finally, the overall contributions of the GDI and PFI gasoline vehicles to ambient particulate matter (PM) were
79 evaluated. This study is part of a project that investigates the relationship between vehicle (engine) emissions and
80 ambient aerosols, including potential of SOA formation from a PFI engine (Du et al., 2017) and the effects of
81 gasoline aromatics on SOA formation (Peng et al., 2017).

82

83 **2 Materials and methods**

84 **2.1 Vehicles**

85 One PFI vehicle and one GDI vehicle were tested in this study to investigate their primary emissions and SOA
86 formations. In this study, the selected PFI and GDI vehicles were certified to the China Phase IV Emissions
87 Standard (equivalent to Euro IV) and the China Phase V Emissions Standard (equivalent to Euro V), respectively.
88 More information of the vehicles is shown in Table 1. **The fuel used in the experiments was a typical Phase V**
89 **gasoline on the China market (sulfur content = 6 mg kg⁻¹). More information of the fuel is provided in Table S1 in**
90 **the Supplement.** Cold-start BJC, characterized by a higher proportion of idling periods and lower acceleration
91 speeds than the New European Driving Cycle (NEDC), was performed to simulate the repeated braking and
92 acceleration on road in megacities such as Beijing. The BJC lasted approximately 17 minutes, with a maximum
93 speed of 50 km h⁻¹ (Peng et al., 2017).

94

95 **2.2 Experimental setup**

96 The chamber experiments were carried out in the summer at the State Key Laboratory of Automotive Safety
97 and Energy of Tsinghua University in Beijing, including two experiments conducted with GDI vehicle and four
98 experiments conducted with PFI vehicle. The tested vehicles were placed on a chassis dynamometer system (Burke
99 E. Porter Machinery Company) with a controlled room temperature and absolute humidity of 26.4±2.5 °C and
100 11.5±2.4 g m⁻³, respectively. The exhaust emitted by the vehicle tailpipe was diluted in a constant volume sampler

101 (CVS) system, where the flow was maintained at $5.5 \text{ m}^3 \text{ min}^{-1}$ using filtered ambient air, achieving about 20 times
102 dilution of the exhaust. Several instruments, including an AVL CEBII gas analyzer, a Cambustion Differential
103 Mobility Spectrometer (DMS500) and a particle sampler, were connected to the CVS (detailed in Figure 1 and
104 section 2.3) to characterize the primary gas- and particulate-phase pollutants. The diluted exhausts produced by the
105 CVS system were injected into an outdoor chamber, where secondary aerosol formation from gasoline vehicle
106 exhausts was simulated. This was the second dilution step of the exhausts and had a dilution factor of approximately
107 15. A schematic illustration of the outdoor experimental setup is shown in Figure 1.

108 The photochemical oxidation experiments were carried out in a quasi-atmospheric aerosol evolution study
109 (QUALITY) outdoor chamber. More details of the setup and performance of the QUALITY chamber were
110 introduced by Peng et al. (2017). Prior to each experiment, the chamber was covered with a double-layer anti-
111 ultraviolet (anti-UV) shade to block sunlight and was cleaned with zero air for about 15 h to create a clean
112 environment. Approximately 120 ppb O_3 were injected into the chamber prior to the injection of vehicle exhaust to
113 make the oxidation environment similar to the mean O_3 peak concentration in the ambient atmosphere. Before the
114 chamber was exposed to sunlight, about 15-minute period was left to ensure that the pollutants mixed sufficiently
115 in the chamber, then the initial concentrations were characterized in the dark. Subsequently, the anti-UV shade
116 were removed from the chamber and photo-oxidation was initiated. A suite of high time resolution instruments was
117 utilized to track the evolution of pollutants during the chamber experiments. Zero air was added into the chamber
118 when sampling to maintain a constant pressure.

119

120 **2.3 Instrumentation**

121 Primary gases and aerosols were measured by the instruments connected to the CVS. The concentrations of
122 gaseous pollutants, including CO , CO_2 , NO_x and total hydrocarbon (THC) were monitored with a gas analyzer
123 AVL Combustion Emissions Bench II (CEB II, AVL, Austria). Primary aerosols were measured with both on-line
124 and off-line instruments. A DMS500 (Cambustion, UK) was implemented to monitor the real-time number size
125 distribution and total number concentration of primary particles. Its sampling line was heated to maintain the

126 temperature at 150°C. The aerosols were also collected on Teflon and quartz filters by AVL Particulate Sampling
127 System (SPC472, AVL, Austria) to analyze the mass, organic carbon (OC) and elemental carbon (EC) emission
128 factors using a balance and OC/EC analyzer (Sunset Lab, USA).

129 During the chamber experiments, a suite of real-time instruments was utilized to characterize the evolutions
130 of the gas and particulate-phase pollutants. CO analyzer, NO-NO₂-NO_x analyzer and O₃ analyzer (Thermo Fisher
131 Scientific Inc., USA) were employed to measure the concentrations of CO, NO_x (including NO and NO₂) and O₃,
132 respectively. The evolutions of volatile organic compounds (VOCs) were monitored with a proton transfer reaction
133 mass spectrometer (PTR-MS, IoniconAnalytik, Austria) (Lindinger et al., 1998). H₃O⁺ was used as the reagent ion,
134 which reacted with the target compounds. The resulting ions were detected by a quadruple mass spectrometer.
135 Meanwhile, the particles size distribution was characterized using a scanning mobility particle sizer system (SMPS,
136 TSI, USA), which consisted of a differential mobility analyzer (DMA, TSI, USA) and a condensation particle
137 counter (CPC, TSI, USA). This system can measure aerosols with a diameters ranging from 15 nm to 700 nm. A
138 high-resolution time-of-flight aerosol mass spectrometer (HR-ToF-AMS, Aerodyne Research, USA) was applied to
139 obtain mass concentrations and size distributions of submicron, non-refractory aerosols, including sulfate, nitrate,
140 ammonium, chloride and organic (DeCarlo et al., 2006). Table 2 lists the instruments used to measure the primary
141 emissions and their evolutions in the chamber experiments.

142

143 **3 Results**

144 **3.1 Primary emissions**

145 **Gaseous pollutant emissions**

146 Emission factors (EFs) of CO₂, THC, benzene and toluene from the GDI and PFI vehicles are listed in Table
147 3. The EFs of CO₂ and THC are derived from measured concentrations in CVS, while the EFs of benzene and
148 toluene were calculated from the initial concentrations in the chamber. The THC emission factor was reported in
149 units of carbon mass, g C kg⁻¹fuel⁻¹.

150 The GDI vehicle emitted less CO₂ and THC than the PFI vehicle due to their different fuel injection strategies

151 and mixing features (Liang et al. 2013; Gao et al., 2015). The EF of THC from the GDI vehicle met the standard
152 of the China Phase V Emission Standard (0.1 g km^{-1}), but that from the PFI vehicle was slightly beyond the standard
153 limit. The PFI vehicle used in this study met lower emission standard (the China Phase IV), which might cause
154 additional THC emission when compared to the China Phase V Emission Standard. In addition, BJC and NEDC
155 were applied in this study and emission standard, respectively. More repeated braking and acceleration in BJC
156 might cause incomplete combustion and consequently higher THC emission from the PFI vehicle in this study. As
157 typical VOC species emitted by vehicles, benzene and toluene were measured in this study. For both vehicles, the
158 EFs of toluene were higher than those of benzene. Consistent with the feature of THC emission, the PFI vehicle
159 emitted more benzene and toluene than the GDI vehicle, and the enhancement of toluene was much larger than that
160 of benzene.

161 The EFs of the gaseous pollutants in this study had similar magnitudes to those in previous studies in which
162 gasoline vehicles met comparable levels of emission standards and were tested under cold-start driving condition,
163 while the results in this study were slightly higher, as shown in Table 3. This difference might be because the
164 California ultralow-emission vehicles (ULEV) (Saliba et al., 2017) and most LEV II vehicles (manufactured in
165 2004 or later) (May et al., 2014) meet the US certification gasoline emission standards for the ULEV category,
166 which has a lower limit of gaseous pollutants than the China Phase V Emission Standard. In addition, the different
167 driving cycles of our study and those other studies (listed in Table 3) might be another explanation for the difference
168 in the EFs of gaseous pollutants.

169 **Primary particle emissions**

170 The EFs of PM, elemental carbon (EC), POA and particulate polycyclic aromatic hydrocarbons (PAHs) are
171 shown in Table 4. The EF of $\text{PM}_{2.5}$ from the GDI vehicle was about 1.4 times higher than that of the PFI vehicle.
172 Both vehicles met the China Phase V Emission Standard for PM emission (4.5 mg km^{-1}). The GDI vehicle emitted
173 about 3.3 times more EC and 1.2 times more POA than the PFI vehicle. The primary carbonaceous aerosols
174 (EC+POA) accounted for 85 % and 82 % of the PM in the GDI and PFI vehicles respectively, suggesting that
175 carbonaceous aerosols were the major contributors in the PM from gasoline vehicles, especially for the GDI vehicle.

PAHs account for a small fraction of particulate organic matter in the atmosphere, but the molecular signature of PAHs can be utilized in source identification of vehicle emissions (Kamal et al., 2015). The GDI vehicle emitted about 1.5 times the PAHs of the PFI vehicle. The EFs of PAH compounds are listed in Table S2 in the Supplement, and details of PAHs measurement was described in Li et al. (2016). It should be noted that the PAHs were tested under warm-start cycles. A higher EF of PAHs would be obtained under cold-start cycle, since the lower temperature led to inefficient catalyst at the beginning of cold-start (Mathis et al., 2005). The main contributors to total PAHs mass emitted from gasoline vehicle exhaust in this study, especially from the GDI vehicle exhaust, was similar with the results reported by previous studies (Schauer et al., 2002; Hays et al., 2013).

The lower PM_{2.5} and POA emissions from GDI vehicle were found in previous studies, except that a little higher PM_{2.5} emission from GDI vehicle was illustrated in Saliba's study (Platt et al., 2013; May et al., 2014; Zhu et al., 2016; Saliba et al., 2017). The EC emissions were in the range of those of previous studies but on the lower level. The EF of the POA measured in this study was higher than those of other studies, leading to a higher OC/EC ratio, which could be attributed to the less strict emission standard of our vehicles and the different driving cycles applied in the experiments.

The bimodal number size distributions of the primary PM from the vehicles measured by the DMS500 are shown in Figure 2. The particle distributions of the exhausts of the GDI and PFI vehicles illustrated similar patterns, with two peaks located at about 10 nm for nucleation mode and at 60-90 nm for accumulation mode, respectively, which are consistent with the results of previous studies (Maricq et al., 1999; Chen et al., 2017). The particle number size distribution of the exhausts of the GDI vehicle showed a similar pattern to that of the PFI vehicle, with a much higher number concentration that is consistent with the emission of more particle mass.

3.2 SOA formation from gasoline vehicle exhaust

The time-resolved concentrations of gases and particles during the chamber experiments are illustrated in Figure 3. Before removing the anti-UV shade, the initial concentrations of NO_x, benzene and toluene from the PFI and GDI vehicles were 80 ppb, 3 ppb, 5 ppb and 100 ppb, 4 ppb, 14 ppb respectively.

After the aging experiment started ($t=0$ in Figure 3), NO was formed from NO₂ photolysis, and then reacted with O₃ to form NO₂. The O₃ concentration increased rapidly to a maximum within 2-3 h and then decreased via reactions and dilution. Benzene and toluene decayed during the aging process at different rates.

New particle formation was found inside the chamber 15 minutes after the exhaust was exposed to sunlight, providing substantial seeds for secondary aerosol formation. Significant growths of particles in both size and mass were observed in the chamber, indicating that a large amount of secondary aerosol was formed during the photochemical oxidation. The chemical compositions of the secondary aerosols were measured continuously by HR-Tof-AMS. Organic was the dominant composition of the secondary aerosol, accounting for 88-95 % of the total particle mass inside the chamber (Figure S1), which is consistent with our previous research (Peng et al., 2017). The SOA mass exhibited different growth rate for the two types of vehicles. After a 4 h oxidation in the chamber, the SOA formed from the exhaust of the GDI vehicle was approximately double that of the PFI vehicle.

The solar radiation conditions significantly influenced the SOA formation. Thus, OH exposure was used to characterize the photochemical age as a normalization, instead of the experiment time. Two VOC species with noticeable differences in their reaction rate constants with OH radicals could be utilized to calculate the OH exposure ($[OH] \Delta t$) based on Equation 1 (for benzene and toluene, as used in this study) (Yuan et al., 2012).

$$[OH] \Delta t = \frac{1}{k_T - k_B} \times \left(\ln \frac{[T]}{[B]} \Big|_{t=0} - \ln \frac{[T]}{[B]} \right) \quad (1)$$

where k_T and k_B are the OH rate constants of benzene ($1.2 \times 10^{-12} \text{ cm}^3 \text{ molecule}^{-1} \text{ s}^{-1}$) (Yuan et al., 2012) and toluene ($5.5 \times 10^{-12} \text{ cm}^3 \text{ molecule}^{-1} \text{ s}^{-1}$) (Kramp and Paulson, 1998), respectively. $\frac{[T]}{[B]} \Big|_{t=0}$ is the concentration ratio of toluene to benzene at the beginning of the aging process, and $\frac{[T]}{[B]}$ is their concentration ratio measured during aging process.

The SOA concentrations as a function of OH exposure are illustrated in Figure 4. Wall-loss correction and dilution correction, including both particles and gaseous pollutants, were taken into consideration in the calculation of the SOA mass concentration in the chamber. Detailed descriptions of corrections are given in the Supplement. Assuming the mean OH concentration was $1.6 \times 10^6 \text{ molecular cm}^{-3}$ in Beijing (Lu et al., 2013), the whole aging

225 procedure in the chamber experiments was equal to a 6-10 h atmospheric photochemical oxidation. The average
226 SOA concentrations were 9.25 ± 1.80 and $4.68 \pm 1.32 \mu\text{g m}^{-3}$ for the GDI and PFI vehicles, respectively, when the
227 OH exposure was 5×10^6 molecular $\text{cm}^{-3} \text{ h}$ in the chamber. Considering the driving cycle mileage and fuel
228 consumption, the SOA productions were $54.77 \pm 10.70 \text{ mg kg-fuel}^{-1}$ or $3.06 \pm 0.60 \text{ mg km}^{-1}$ for the GDI vehicle and
229 $20.57 \pm 5.82 \text{ mg kg-fuel}^{-1}$ or $1.55 \pm 0.44 \text{ mg km}^{-1}$ for the PFI vehicle. Compared with the PFI vehicle, the GDI vehicle
230 exhaust exhibited a higher potential of SOA formation, even though the PFI vehicle emitted more VOCs, which
231 are considered as dominant class of SOA precursors. This result indicates that higher concentrations of some other
232 SOA precursors exist in the exhaust of GDI vehicles, which will be further discussed in section 3.3.

233 The results from chamber simulation of SOA formation from individual gasoline vehicles are illustrated in
234 Figure 5. The SOA production from the both vehicles in this study is in the range of the results of previous studies
235 (Nordin et al., 2013; Platt et al., 2013; Jathar et al., 2014; Liu et al., 2015; Peng et al., 2017). The variation of the
236 SOA production among these studies might be caused by several factors: the model years of vehicles
237 (corresponding to emission standards) (Nordin et al., 2013; Liu et al., 2015), their driving cycles (Nordin et al.,
238 2013), the initial concentrations of gaseous pollutants in the chamber (Jathar et al., 2014), and the ratio of VOCs to
239 NO_x (Zhao et al., 2017) in the chamber experiments.

240 To investigate the dominant contributors to ambient PM from the GDI and PFI vehicles, Figure 6 illustrates
241 the EFs of EC and POA as well as the production factors of SOA in this study. The SOA production from the GDI
242 vehicle was approximately 2.7 times higher than that from the PFI vehicle. At 5×10^6 molecular $\text{cm}^{-3} \text{ h}$ OH exposure,
243 the SOA/POA ratio was approximately 1. Figure 4 illustrates that the SOA production increased with
244 photochemical age rapidly (within 2×10^7 molecular $\text{cm}^{-3} \text{ h}$). Thus, SOA would exceed POA at higher OH exposure,
245 e.g., the SOA/POA ratio reached about 4 at 10^7 molecular $\text{cm}^{-3} \text{ h}$ OH exposure, becoming the major PM contributor.
246 In terms of the POA and EC emissions as well as the SOA formation, the GDI vehicle contributed 2.2 times more
247 than the PFI vehicle.

248 Although particle wall-loss correction as well as particle and gas dilution corrections were considered in this
249 study, several factors may still contribute to the uncertainties of the SOA productions. First, the deposition of semi-

volatile vapors to the chamber walls was not corrected, which may result in an underestimation of the rate of SOA production with a factor of 1.1-4.1 (Zhang et al., 2014). Second, under some ambient conditions such as severe urban haze events (Guo et al., 2014), particle mass concentrations can be as high as 200-300 $\mu\text{g m}^{-3}$, much higher than the $23 \pm 6 \mu\text{g m}^{-3}$ under the chamber condition in this study. High particle mass loadings are favorable for the partition of semi-volatile compounds into the particle phase, potentially increasing the rate of SOA production (Odum et al., 1996). Third, stronger partitioning of SOA precursors into the particle phase may reduce the oxidized products in the gas phase, which will potentially reduce the rate of SOA production (Seinfeld et al., 2003)

3.3 SOA mass closure

SOA production ($\Delta\text{OA}_{\text{predicted}}$) estimated from VOC precursors can be defined as Eq. (2):

$$\Delta\text{OA}_{\text{predicted}} = \sum_i (\Delta_i \times Y_i) \quad (2)$$

where Δ_i is the concentration change of precursor VOC_i measured with PTR-MS in the chamber experiments, and Y_i is the SOA yield of the VOC_i . In this study, benzene, toluene, C8 benzene and C9 benzene were involved in the estimation of SOA production, and alkanes and alkenes were not considered. A recent study found that ozonolysis of alkenes from gasoline vehicle exhaust could form SOA through aldol condensation reactions (Yang et al., 2018). However, much low declines of concentrations were observed than those of aromatics during chamber experiments, so alkenes might not play significant role in SOA formation in this study.

The SOA yield is sensitive to VOCs/ NO_x ratio (Song et al., 2005). In this study, the VOCs/ NO_x ratio was in the range of 0.5-1.0 ppbC/ppb, thus, the SOA formation from the vehicle exhaust was determined under high NO_x conditions. The high NO_x SOA yields of benzene and toluene were taken from Ng et al. (2007). The C8 and C9 benzene used the SOA yield of m-xylene from Platt et al. (2013).

The increased predicted SOA contribution from the VOC precursors as a function of OH exposure accumulation is demonstrated in Figure 7. At the end of the experiments, the SOA estimated from these speciated VOCs accounted for about 25 % and 53 % of the measured SOA formation from the GDI and PFI vehicle exhausts, respectively. Similar to the results of previous studies (Platt et al., 2013; Nordin et al., 2013; Gordon et al., 2014),

single-ring aromatics played an important role in the SOA formation, especially for the PFI vehicle which shows higher predicted SOA fraction.

The unpredicted fraction of the measured SOA in the chamber experiments was in the range of 47-75 %. Contributions from intermediate volatility organic compounds (IVOCs) and semivolatile organic compounds (SVOCs), e.g., long branched and cyclic alkanes and gas-phase polycyclic aromatic hydrocarbons could be a possible explanation for this underestimation. The SOA formed by oxidation of IVOCs and SVOCs is found to dominate over that from single-ring aromatics (Robinson et al., 2007; Zhao et al., 2016). The unpredicted SOA ratio exhibited a maximum value at the beginning of the experiment, indicating that the IVOCs and SVOCs with low volatilities produced SOA much more efficiently than the single-ring aromatics with high volatilities, as the first generation products of photo-oxidation of these precursors form SOA (Robinson et al., 2007).

The larger fraction of the unpredicted SOA from the GDI vehicle exhaust might be associated with higher IVOCs and SVOCs emissions. Gas-phase PAH is one of the main component of speciated IVOCs (Zhao et al., 2016). The particulate-phase PAHs from the GDI vehicle were more abundant than those from the PFI vehicle by a factor of 1.5 (section 3.1). Based on gas-particle equilibrium, this indicates that more gas-phase PAHs, including some aromatic IVOCs, might be emitted by the GDI vehicles, contributing to the SOA enhancement.

290

291 **4 Discussions and conclusions**

GDI and PFI vehicles have different fuel injection technologies in their engines, which affects their emissions of gaseous and particulate pollutants. In GDI engine, the fuel is directly injected into cylinder, which benefits the fuel atomization and vaporization and provides better control of fuel volume and the combustion process (Liang et al. 2013; Gao et al., 2015). Thus, in this study, the tested GDI vehicle has higher fuel economy and lower THC emission than the PFI vehicle. However, the insufficient mixing time allowed for the fuel and air leads to incomplete combustion in the GDI engine (Fu et al., 2014). In addition, direct fuel injection leads to fuel impingement onto surfaces of combustion chamber, where liquid pools form, favoring soot-like particulate formation (Ueberall et al., 2015; Chen et al., 2017). Consequently, larger particle mass and number are emitted by

the GDI vehicle than from the PFI vehicle. The particles emitted by the GDI vehicle have higher EC mass fraction, leading to lower OC/EC ratio. The considerable particle number emitted by gasoline vehicles, especially in GDI vehicles exhaust, makes a significant contribution to particle number concentration as well as seeds for further reactions in the atmosphere, and needs to be controlled in the future emission standards.

Our results show that the GDI vehicle contributes more to both primary and secondary aerosol than the PFI vehicle, and has greater impact on environment and air quality. In recent years, the market share of GDI vehicles exerts a continuous growth in China because they provide better fuel economy and lower CO₂ emissions. In 2016, GDI vehicles accounted for 25 % of China's market share in sales, and this proportion is expected to reach 60 % by 2020 (Wen et al., 2016). The PM enhancement of GDI vehicles with increasing population could potentially offset any PM emission reduction benefits, including the development of gasoline emission and fuel standards and the advanced engine technologies of gasoline vehicles. Therefore, our results highlight the necessity of further research and regulation of GDI vehicles.

It should be pointed out that the SOA formation factors in this study are based on one GDI vehicle and one PFI vehicle. Some previous studies proposed that vehicles have variations even though they meet similar specification vehicles and use the same fuel (Gordon et al., 2014; Jathar et al., 2014). Thus more researches with more vehicles for each technology are needed on SOA formation from vehicle exhaust.

Primary emissions and secondary organic formation from one GDI vehicle and one PFI vehicle were investigated when driving under cold-start BJC. The primary PM emitted by the GDI vehicle was 1.4 times greater than that from the PFI vehicle and the SOA formation from the GDI vehicle exhaust was 2.7 times greater than that from the PFI vehicle exhaust for the same OH exposure. The SOA production factors were $54.77 \pm 10.70 \text{ mg kg}^{-1} \text{ fuel}^{-1}$ or $3.06 \pm 0.60 \text{ mg km}^{-1}$ for the GDI vehicle and $20.57 \pm 5.82 \text{ mg kg-fuel}^{-1}$ or $1.55 \pm 0.44 \text{ mg km}^{-1}$ for the PFI vehicle at an OH exposure of $5 \times 10^6 \text{ molecular cm}^{-3} \text{ h}$, which is consistent with the values seen in previous studies. Considering the higher amounts of OA derived from primary emission and secondary formation, the GDI vehicle contribute considerably more to particle mass concentrations in the ambient air than the PFI vehicle.

The SOA formation was predicted from the gaseous precursors emitted by the GDI and PFI vehicles under

325 high NO_x condition. Single-ring aromatic VOCs could explain only 25-53 % of the measured SOA formation in
326 the chamber experiments. The GDI vehicle exhibited higher fraction of unexplained SOA. More IVOCs and
327 SVOCs were inferred as being emitted by the GDI vehicle.

328 With increasing population of GDI vehicles, any benefits of the aerosol emission reduction of gasoline
329 vehicles are substantially offset, because GDI vehicles have significant contributions to ambient aerosols. More
330 work is needed to improve the understanding of GDI vehicle emissions and to provide information for the
331 regulation of gasoline vehicles.

332

333

334 *Data availability.* The data presented in this article are available from the authors upon request
335 (minhu@pku.edu.cn).

336

337

338 **Acknowledgments**

339 This work was supported by the National Basic Research Program of China (973 Program) (2013CB228503,
340 2013CB228502), National Natural Science Foundation of China (91544214, 41421064, 51636003), the Strategic
341 Priority Research Program of Chinese Academy of Sciences (XDB05010500), and China Postdoctoral Science
342 Foundation (2015M580929). We also thank the State Key Lab of Automotive Safety and Energy at Tsinghua
343 University for the support to experiments.

344

345 **Reference**

346 **Alkidas, A. C.: Combustion advancements in gasoline engines, *Energy Conversion and Management*, 48, 2751-**
347 **2761, [10.1016/j.enconman.2007.07.027](https://doi.org/10.1016/j.enconman.2007.07.027), 2007.**

348 Bahreini, R., Middlebrook, A. M., de Gouw, J. A., Warneke, C., Trainer, M., Brock, C. A., Stark, H., Brown, S. S.,
349 Dube, W. P., Gilman, J. B., Hall, K., Holloway, J. S., Kuster, W. C., Perring, A. E., Prevot, A. S. H., Schwarz, J. P.,
350 Spackman, J. R., Szidat, S., Wagner, N. L., Weber, R. J., Zotter, P., and Parrish, D. D.: Gasoline emissions dominate
351 over diesel in formation of secondary organic aerosol mass, *Geophysical Research Letters*, 39,
352 10.1029/2011gl050718, 2012.

353 Chen, L., Liang, Z., Zhang, X., and Shuai, S.: Characterizing particulate matter emissions from GDI and PFI
354 vehicles under transient and cold start conditions, *Fuel*, 189, 131-140, [10.1016/j.fuel.2016.10.055](https://doi.org/10.1016/j.fuel.2016.10.055), 2017.

355 DeCarlo, P. F., Kimmel, J. R., Trimborn, A., Northway, M. J., Jayne, J. T., Aiken, A. C., Gonin, M., Fuhrer, K.,
356 Horvath, T., Docherty, K. S., Worsnop, D. R., and Jimenez, J. L.: Field-deployable, high-resolution, time-of-flight
357 aerosol mass spectrometer, *Analytical Chemistry*, 78, 8281-8289, [10.1021/ac061249n](https://doi.org/10.1021/ac061249n), 2006.

358 Du, Z., Hu, M., Peng, J., Guo, S., Zheng, R., Zheng, J., Shang, D., Qin, Y., Niu, H., Li, M., Yang, Y., Lu, S., Wu,
359 Y., Shao, M., and Shuai, S.: Potential of secondary aerosol formation from Chinese gasoline engine exhaust, *Journal*
360 *of environmental sciences*, 2017, in press.

361 Fu, H., Wang, Y., Li, X., and Shuai, S.: Impacts of Cold-Start and Gasoline RON on Particulate Emission from
362 Vehicles Powered by GDI and PFI Engines, *SAE Technical Paper*, 2014-01-2836, [10.4271/2014-01-2836](https://doi.org/10.4271/2014-01-2836), 2014.

363 Gao, Z., Curran, S. J., Parks, J. E., II, Smith, D. E., Wagner, R. M., Daw, C. S., Edwards, K. D., and Thomas, J. F.:
364 Drive cycle simulation of high efficiency combustions on fuel economy and exhaust properties in light-duty
365 vehicles, *Applied Energy*, 157, 762-776, [10.1016/j.apenergy.2015.03.070](https://doi.org/10.1016/j.apenergy.2015.03.070), 2015.

366 Gentner, D. R., Jathar, S. H., Gordon, T. D., Bahreini, R., Day, D. A., El Haddad, I., Hayes, P. L., Pieber, S. M.,
367 Platt, S. M., de Gouw, J., Goldstein, A. H., Harley, R. A., Jimenez, J. L., Prevot, A. S. H., and Robinson, A. L.:
368 Review of Urban Secondary Organic Aerosol Formation from Gasoline and Diesel Motor Vehicle Emissions,
369 *Environmental science & technology*, 51, 1074-1093, [10.1021/acs.est.6b04509](https://doi.org/10.1021/acs.est.6b04509), 2017.

370 Gordon, T. D., Presto, A. A., May, A. A., Nguyen, N. T., Lipsky, E. M., Donahue, N. M., Gutierrez, A., Zhang, M.,
 371 Maddox, C., Rieger, P., Chattopadhyay, S., Maldonado, H., Maricq, M. M., and Robinson, A. L.: Secondary organic
 372 aerosol formation exceeds primary particulate matter emissions for light-duty gasoline vehicles, *Atmos. Chem.*
 373 *Phys.* , 14, 4661-4678, 10.5194/acp-14-4661-2014, 2014.
 374 Guo, S., Hu, M., Zamora, M. L., Peng, J., Shang, D., Zheng, J., Du, Z., Wu, Z., Shao, M., Zeng, L., Molina, M. J.,
 375 and Zhang, R.: Elucidating severe urban haze formation in China, *Proceedings of the National Academy of*
 376 *Sciences of the United States of America*, 111, 17373-17378, 10.1073/pnas.1419604111, 2014.
 377 Hayes, P. L., Ortega, A. M., Cubison, M. J., Froyd, K. D., Zhao, Y., Cliff, S. S., Hu, W. W., Toohey, D. W., Flynn,
 378 J. H., Lefer, B. L., Grossberg, N., Alvarez, S., Rappenglueck, B., Taylor, J. W., Allan, J. D., Holloway, J. S., Gilman,
 379 J. B., Kuster, W. C., De Gouw, J. A., Massoli, P., Zhang, X., Liu, J., Weber, R. J., Corrigan, A. L., Russell, L. M.,
 380 Isaacman, G., Worton, D. R., Kreisberg, N. M., Goldstein, A. H., Thalman, R., Waxman, E. M., Volkamer, R., Lin,
 381 Y. H., Surratt, J. D., Kleindienst, T. E., Offenberg, J. H., Dusanter, S., Griffith, S., Stevens, P. S., Brioude, J.,
 382 Angevine, W. M., and Jimenez, J. L.: Organic aerosol composition and sources in Pasadena, California, during the
 383 2010 CalNex campaign, *Journal of Geophysical Research-Atmospheres*, 118, 9233-9257, 10.1002/jgrd.50530,
 384 2013.
 385 Hays, M. D., Preston, W., George, B. J., Schmid, J., Baldauf, R., Snow, R., Robinson, J. R., Long, T., and Faircloth,
 386 J.: Carbonaceous aerosols emitted from light-duty vehicles operating on gasoline and ethanol fuel blends,
 387 *Environmental science & technology*, 47, 14502-14509, 10.1021/es403096v, 2013.
 388 Hu, W., Hu, M., Hu, W., Jimenez, J. L., Yuan, B., Chen, W., Wang, M., Wu, Y., Chen, C., Wang, Z., Peng, J., Zeng,
 389 L., and Shao, M.: Chemical composition, sources, and aging process of submicron aerosols in Beijing: Contrast
 390 between summer and winter, *Journal of Geophysical Research-Atmospheres*, 121, 1955-1977,
 391 10.1002/2015jd024020, 2016.
 392 Huang, R.-J., Zhang, Y., Bozzetti, C., Ho, K.-F., Cao, J.-J., Han, Y., Daellenbach, K. R., Slowik, J. G., Platt, S. M.,
 393 Canonaco, F., Zotter, P., Wolf, R., Pieber, S. M., Bruns, E. A., Crippa, M., Ciarelli, G., Piazzalunga, A.,
 394 Schwikowski, M., Abbaszade, G., Schnelle-Kreis, J., Zimmermann, R., An, Z., Szidat, S., Baltensperger, U.,

395 Haddad, I. E., and Prévôt, A. S. H.: High secondary aerosol contribution to particulate pollution during haze events
 396 in China, *Nature*, 10.1038/nature13774, 2014.

397 Ito, Y., Shimoda, T., Aoki, T., Yuuki, K., Sakamoto, H., Kato, K., Their, D., Kattouah, P., Ohara, E. and Vogt, C.:
 398 Next Generation of Ceramic Wall Flow Gasoline Particulate Filter with Integrated Three Way Catalyst, *SAE*
 399 *Technical Paper 2015-01-1073*, 2015, doi:10.4271/2015-01-1073, 2015.

400 Jathar, S. H., Gordon, T. D., Hennigan, C. J., Pye, H. O. T., Pouliot, G., Adams, P. J., Donahue, N. M., and Robinson,
 401 A. L.: Unspeciated organic emissions from combustion sources and their influence on the secondary organic aerosol
 402 budget in the United States, *Proc. Natl. Acad. Sci. USA*, 111, 10473-10478, 10.1073/pnas.1323740111, 2014.

403 Jathar, S. H., Woody, M., Pye, H. O. T., Baker, K. R., and Robinson, A. L.: Chemical transport model simulations
 404 of organic aerosol in southern California: model evaluation and gasoline and diesel source contributions,
 405 *Atmospheric Chemistry and Physics*, 17, 4305-4318, 10.5194/acp-17-4305-2017, 2017.

406 Kamal, A., Cincinelli, A., Martellini, T., and Malik, R. N.: A review of PAH exposure from the combustion of
 407 biomass fuel and their less surveyed effect on the blood parameters, *Environmental Science and Pollution Research*,
 408 22, 4076-4098, 10.1007/s11356-014-3748-0, 2015.

409 Kanakidou, M., Seinfeld, J. H., Pandis, S. N., Barnes, I., Dentener, F. J., Facchini, M. C., Van Dingenen, R., Ervens,
 410 B., Nenes, A., Nielsen, C. J., Swietlicki, E., Putaud, J. P., Balkanski, Y., Fuzzi, S., Horth, J., Moortgat, G. K.,
 411 Winterhalter, R., Myhre, C. E. L., Tsigaridis, K., Vignati, E., Stephanou, E. G., and Wilson, J.: Organic aerosol and
 412 global climate modelling: a review, *Atmospheric Chemistry and Physics*, 5, 1053-1123, 2005.

413 Kramp, F., and Paulson, S. E.: On the uncertainties in the rate coefficients for OH reactions with hydrocarbons, and
 414 the rate coefficients of the 1,3,5-trimethylbenzene and m-xylene reactions with OH radicals in the gas phase,
 415 *Journal of Physical Chemistry A*, 102, 2685-2690, 10.1021/jp973289o, 1998.

416 Li, M., Hu, M., Wu, Y., Qin, Y., Zheng, R., Peng, J., Guo, Q., Xiao, Y., Hu, W., Zheng, J., Du, Z., Xiao, J., Shuai,
 417 S.: Characteristics of Particulate Organic Matters Emissions from Gasoline Direct Injection Engine and Its
 418 Influence Factors, *Proceedings of the Chinese Society of Electrical Engineering*, 36, 4443-4451.

419 Liang, B., Ge, Y., Tan, J., Han, X., Gao, L., Hao, L., Ye, W., and Dai, P.: Comparison of PM emissions from a
 420 gasoline direct injected (GDI) vehicle and a port fuel injected (PFI) vehicle measured by electrical low pressure
 421 impactor (ELPI) with two fuels: Gasoline and M15 methanol gasoline, *Journal of Aerosol Science*, 57, 22-31,
 422 10.1016/j.jaerosci.2012.11.008, 2013.

423 Lindinger, W., Hansel, A., and Jordan, A.: On-line monitoring of volatile organic compounds at pptv levels by
 424 means of proton-transfer-reaction mass spectrometry (PTR-MS) - Medical applications, food control and
 425 environmental research, *International Journal of Mass Spectrometry*, 173, 191-241, 10.1016/s0168-
 426 1176(97)00281-4, 1998.

427 Liu, T., Wang, X., Deng, W., Hu, Q., Ding, X., Zhang, Y., He, Q., Zhang, Z., Lü S., Bi, X., Chen, J., and Yu, J.:
 428 Secondary organic aerosol formation from photochemical aging of light-duty gasoline vehicle exhausts in a smog
 429 chamber, *Atmos. Chem. Phys.*, 15, 9049-9062, 10.5194/acp-15-9049-2015, 2015.

430 Lu, K. D., Hofzumahaus, A., Holland, F., Bohn, B., Brauers, T., Fuchs, H., Hu, M., Häsel, R., Kita, K., Kondo,
 431 Y., Li, X., Lou, S. R., Oebel, A., Shao, M., Zeng, L. M., Wahner, A., Zhu, T., Zhang, Y. H., and Rohrer, F.: Missing
 432 OH source in a suburban environment near Beijing: observed and modelled OH and HO₂
 433 concentrations in summer 2006, *Atmos. Chem. Phys.*, 13, 1057-1080, 10.5194/acp-13-1057-2013, 2013.

434 Maricq, M. M., Podsiadlik, D. H., and Chase, R. E.: Gasoline vehicle particle size distributions: Comparison of
 435 steady state, FTP, and US06 measurements, *Environmental science & technology*, 33, 2007-2015,
 436 10.1021/es981005n, 1999.

437 Mathis, U., Mohr, M., and Forss, A. M.: Comprehensive particle characterization of modern gasoline and diesel
 438 passenger cars at low ambient temperatures, *Atmospheric Environment*, 39, 107-117,
 439 10.1016/j.atmosenv.2004.09.029, 2005.

440 May, A. A., Nguyen, N. T., Presto, A. A., Gordon, T. D., Lipsky, E. M., Karve, M., Gutierrez, A., Robertson, W. H.,
 441 Zhang, M., Brandow, C., Chang, O., Chen, S., Cicero-Fernandez, P., Dinkins, L., Fuentes, M., Huang, S.-M., Ling,
 442 R., Long, J., Maddox, C., Massetti, J., McCauley, E., Miguel, A., Na, K., Ong, R., Pang, Y., Rieger, P., Sax, T., Tin,
 443 T., Thu, V., Chattopadhyay, S., Maldonado, H., Maricq, M. M., and Robinson, A. L.: Gas- and particle-phase

primary emissions from in-use, on-road gasoline and diesel vehicles, *Atmospheric Environment*, 88, 247-260, 10.1016/j.atmosenv.2014.01.046, 2014.

Myung, C.-L., Kim, J., Choi, K., Hwang, I. G., and Park, S.: Comparative study of engine control strategies for particulate emissions from direct injection light-duty vehicle fueled with gasoline and liquid phase liquefied petroleum gas (LPG), *Fuel*, 94, 348-355, 10.1016/j.fuel.2011.10.041, 2012.

Ng, N. L., Kroll, J. H., Chan, A. W. H., Chhabra, P. S., Flagan, R. C., and Seinfeld, J. H.: Secondary organic aerosol formation from m-xylene, toluene, and benzene, *Atmos. Chem. Phys.*, 7, 3909–3922, 2007.

Nordin, E. Z., Eriksson, A. C., Roldin, P., Nilsson, P. T., Carlsson, J. E., Kajos, M. K., Hellén, H., Wittbom, C., Rissler, J., Löndahl, J., Swietlicki, E., Svenningsson, B., Bohgard, M., Kulmala, M., Hallquist, M., and Pagels, J. H.: Secondary organic aerosol formation from idling gasoline passenger vehicle emissions investigated in a smog chamber, *Atmos. Chem. Phys.*, 13, 6101-6116, 10.5194/acp-13-6101-2013, 2013.

Odum, J. R., Hoffmann, T., Bowman, F., Collins, D., Flagan, R. C., and Seinfeld, J. H.: Gas/particle partitioning and secondary organic aerosol yields, *Environ. Sci. Technol.*, 30, 2580-2585, 10.1021/es950943+, 1996.

Peng, J., Hu, M., Du, Z., Wang, Y., Zheng, J., Zhang, W., Yang, Y., Qin, Y., Zheng, R., Xiao, Y., Wu, Y., Lu, S., Wu, Z., Guo, S., Mao, H., and Shuai, S.: Gasoline aromatic: a critical determinant of urban secondary organic aerosol formation, *Atmospheric Chemistry and Physics*, 2017, in press.

Platt, S. M., El Haddad, I., Zardini, A. A., Clairotte, M., Astorga, C., Wolf, R., Slowik, J. G., Temime-Roussel, B., Marchand, N., Ježek, I., Drinovec, L., Močnik, G., Möhler, O., Richter, R., Barmet, P., Bianchi, F., Baltensperger, U., and Prévôt, A. S. H.: Secondary organic aerosol formation from gasoline vehicle emissions in a new mobile environmental reaction chamber, *Atmos. Chem. Phys.*, 13, 9141-9158, 10.5194/acp-13-9141-2013, 2013.

Robinson, A. L., Donahue, N. M., Shrivastava, M. K., Weitkamp, E. A., Sage, A. M., Grieshop, A. P., Lane, T. E., Pierce, J. R., and Pandis, S. N.: Rethinking organic aerosols: Semivolatile emissions and photochemical aging, *Science*, 315, 1259-1262, 10.1126/science.1133061, 2007.

Saliba, G., Saleh, R., Zhao, Y., Presto, A. A., Lambe, A. T., Frodin, B., Sardar, S., Maldonado, H., Maddox, C., May, A. A., Drozd, G. T., Goldstein, A. H., Russell, L. M., Hagen, F., and Robinson, A. L.: Comparison of Gasoline

469 Direct-Injection (GDI) and Port Fuel Injection (PFI) Vehicle Emissions: Emission Certification Standards, Cold-
470 Start, Secondary Organic Aerosol Formation Potential, and Potential Climate Impacts, *Environmental science &*
471 *technology*, 51, 6542-6552, 10.1021/acs.est.6b06509, 2017.

472 Schauer, J. J., Kleeman, M. J., Cass, G. R. and Simoneit, B. R. T.: Measurement of Emissions from Air Pollution
473 Sources. 5. C1-C32 Organic Compounds from Gasoline-Powered Motor Vehicles, *Environmental science &*
474 *technology*, 36, 1169-1180, 2002.

475 Seinfeld, J. H., Kleindienst, T. E., Edney, E. O., and Cohen, J. B.: Aerosol growth in a steady-state, continuous flow
476 chamber: Application to studies of secondary aerosol formation, *Aerosol Science and Technology*, 37, 728-734,
477 10.1080/02786820390214954, 2003.

478 Song, C., Na, K. S., and Cocker, D. R.: Impact of the hydrocarbon to NO_x ratio on secondary organic aerosol
479 formation, *Environ. Sci. Technol.*, 39, 3143-3149, 10.1021/es0493244, 2005.

480 Ueberall, A., Otte, R., Eilts, P., and Krahel, J.: A literature research about particle emissions from engines with direct
481 gasoline injection and the potential to reduce these emissions, *Fuel*, 147, 203-207, 10.1016/j.fuel.2015.01.012,
482 2015.

483 Wang, Y., Zheng, R., Qin, Y., Peng, J., Li, M., Lei, J., Wu, Y., Hu, M., and Shuai, S.: The impact of fuel compositions
484 on the particulate emissions of direct injection gasoline engine, *Fuel*, 166, 543-552, 10.1016/j.fuel.2015.11.019,
485 2016.

486 Wang, Z. B., Hu, M., Wu, Z. J., Yue, D. L., He, L. Y., Huang, X. F., Liu, X. G., and Wiedensohler, A.: Long-term
487 measurements of particle number size distributions and the relationships with air mass history and source
488 apportionment in the summer of Beijing, *Atmospheric Chemistry and Physics*, 13, 10159-10170, 10.5194/acp-13-
489 10159-2013, 2013.

490 Wen, Y., Wang, Y., Fu, C., Deng, W., Zhan, Z., Tang, Y., Li, X., Ding, H., and Shuai, S.: The Impact of Injector
491 Deposits on Spray and Particulate Emission of Advanced Gasoline Direct Injection Vehicle, *SAE Technical Paper*,
492 2016-01-2284, 10.4271/2016-01-2284, 2016.

493 Yang, B., Ma, P. K., Shu, J. N., Zhang, P., Huang, J. Y. and Zhang, H. X.: Formation mechanism of secondary
 494 organic aerosol from ozonolysis of gasoline vehicle exhaust, *Environmental Pollution*, 234, 960-968,
 495 10.1016/j.envpol.2017.12.048, 2018.

496 Yuan, B., Shao, M., de Gouw, J., Parrish, D. D., Lu, S., Wang, M., Zeng, L., Zhang, Q., Song, Y., Zhang, J., and
 497 Hu, M.: Volatile organic compounds (VOCs) in urban air: How chemistry affects the interpretation of positive
 498 matrix factorization (PMF) analysis, *Journal of Geophysical Research: Atmospheres*, 117, n/a-n/a,
 499 10.1029/2012jd018236, 2012.

500 Zhang, Q., Jimenez, J. L., Canagaratna, M. R., Allan, J. D., Coe, H., Ulbrich, I., Alfarra, M. R., Takami, A.,
 501 Middlebrook, A. M., Sun, Y. L., Dzepina, K., Dunlea, E., Docherty, K., DeCarlo, P. F., Salcedo, D., Onasch, T.,
 502 Jayne, J. T., Miyoshi, T., Shimo, A., Hatakeyama, S., Takegawa, N., Kondo, Y., Schneider, J., Drewnick, F.,
 503 Borrmann, S., Weimer, S., Demerjian, K., Williams, P., Bower, K., Bahreini, R., Cottrell, L., Griffin, R. J.,
 504 Rautiainen, J., Sun, J. Y., Zhang, Y. M., and Worsnop, D. R.: Ubiquity and dominance of oxygenated species in
 505 organic aerosols in anthropogenically-influenced Northern Hemisphere midlatitudes, *Geophysical Research Letters*,
 506 34, 10.1029/2007gl029979, 2007.

507 Zhang, X., Cappa, C. D., Jathar, S. H., McVay, R. C., Ensberg, J. J., Kleeman, M. J., and Seinfeld, J. H.: Influence
 508 of vapor wall loss in laboratory chambers on yields of secondary organic aerosol, *Proc. Natl. Acad. Sci. USA*, 111,
 509 5802-5807, 10.1073/pnas.1404727111, 2014.

510 Zhao, Y., Nguyen, N. T., Presto, A. A., Hennigan, C. J., May, A. A., and Robinson, A. L.: Intermediate Volatility
 511 Organic Compound Emissions from On-Road Gasoline Vehicles and Small Off-Road Gasoline Engines,
 512 *Environmental science & technology*, 50, 4554-4563, 10.1021/acs.est.5b06247, 2016.

513 Zhao, Y., Saleh, R., Saliba, G., Presto, A. A., Gordon, T. D., Drozd, G. T., Goldstein, A. H., Donahue, N. M., and
 514 Robinson, A. L.: Reducing secondary organic aerosol formation from gasoline vehicle exhaust, *Proceedings of the
 515 National Academy of Sciences of the United States of America*, 114, 6984-6989, 10.1073/pnas.1620911114, 2017.

516 Zhu, R., Hu, J., Bao, X., He, L., Lai, Y., Zu, L., Li, Y., and Su, S.: Tailpipe emissions from gasoline direct injection
517 (GDI) and port fuel injection (PFI) vehicles at both low and high ambient temperatures, *Environmental Pollution*,
518 216, 223-234, 10.1016/j.envpol.2016.05.066, 2016.

519 Zimmerman, N., Wang, J. M., Jeong, C.-H., Ramos, M., Hilker, N., Healy, R. M., Sabaliauskas, K., Wallace, J. S.,
520 and Evans, G. J.: Field Measurements of Gasoline Direct Injection Emission Factors: Spatial and Seasonal
521 Variability, *Environmental science & technology*, 50, 2035-2043, 10.1021/acs.est.5b04444, 2016.

522

523 Table 1 Descriptions of the gasoline direct injection (GDI) and port fuel injection (PFI) vehicles used in the
524 experiments.

Vehicle	Make and model	Emission standard class	Model year	Mileage (km)	Displacement (cm ³)	Power (kW)	Weight (kg)
GDI	VW Sagitar	China V	2015	3000	1395	110	1395
PFI	Honda Civic	China IV	2009	42500	1799	103	1280

525

526

Table 2 Overview of all instruments used to measure the gas and particulate phase pollutants in the experiments.

Parameter	Phase	Instrument	Note
CO, CO ₂ , NO _x and total hydrocarbon (THC) concentration	Gas	Gas analyzer AVL Combustion Emissions Bench II	On-line
Aerosol number size distribution	Particle	DMS500	On-line
PM _{2.5}	Particle	Balance (AX105DR)	Off-line
Organic carbon/Elemental carbon concentration	Particle	OC/EC analyzer	Off-line
CO concentration	Gas	48i CO analyzer	On-line
NO, NO ₂ , and NO _x concentration	Gas	42i NO-NO ₂ -NO _x analyzer	On-line
O ₃ concentration	Gas	49i O ₃ analyzer	On-line
VOCs concentration	Gas	Proton transfer reaction mass spectrometer (PTR-MS)	On-line
Aerosol number (mass) size distribution	Particle	Scanning mobility particle sizer (SMPS, consist of 3081-DMA and 3775-CPC),	On-line
Size resolved non-refractory aerosol	Particle	High resolution time-of-flight aerosol mass spectrometer (HR-Tof-AMS)	On-line

527

528

529

Table 3 Emission factors (EFs) of gaseous pollutants from the gasoline direct injection (GDI) and port fuel injection (PFI) vehicles in

530

this study and those of previous studies.

	This study				Saliba et al., 2017		May et al., 2014	Platt et al., 2013		Zhu et al., 2016	
	GDI		PFI		GDI	PFI	PFI ^a			GDI	PFI
	China V		China IV		ULEV	ULEV	LEV II	Euro V		China IV	China IV
	Cold BJC				Cold UC ^b		Cold UC	Cold NEDC		Cold WLTC ^c	
	g kg- fuel ⁻¹	g km ⁻¹	g kg- fuel ⁻¹	g km ⁻¹	g km ⁻¹	g km ⁻¹	g kg-fuel ⁻¹	g kg-fuel ⁻¹	g km ⁻¹	g km ⁻¹	g km ⁻¹
CO ₂	3439	213	3350	283	-	-	-	-	-	187	215
	±23	±4	±24	±4							
THC	1.55	0.09	1.70	0.13	0.02	0.06	0.64	0.91-1.06	0.036-	0.05	0.03
	±0.22	±0.01	±0.19	±0.01					0.042		
Benzene	0.056	0.003	0.061	0.005	-	-	0.018	-	0.002	-	-
	±0.011	±0.001	±0.016	±0.001							
Toluene	0.101	0.006	0.220	0.017	-	-	0.026	-	0.002	-	-
	±0.004	±0.001	±0.047	±0.004							

531

^a 22 PFI vehicles and 3 GDI vehicles;

532

^b UC: Unified Cycle;

533

^c WLTC: Worldwide-harmonized Light-duty Test Cycle

534 Table 4 EFs of primary aerosols, including carbonaceous aerosols and particulate polycyclic aromatic hydrocarbons (PAHs) from the
535 GDI and PFI vehicles in this study and those of previous studies.

	This study				Saliba et al., 2017		May et al., 2014	Platt et al., 2013		Zhu et al., 2016	
	GDI		PFI		GDI	PFI	PFI			GDI	PFI
	China V		China IV		ULEV	ULEV	LEV II	Euro V		China IV	China IV
	Cold BJC				Cold UC		Cold UC	Cold NEDC		Cold WLTC	
	mg kg-	mg km ⁻¹	mg kg-	mg km ⁻¹	mg km ⁻¹	mg km ⁻¹	mg kg-fuel ⁻¹	mg kg-	mg km ⁻¹	mg km ⁻¹	mg km ⁻¹
	fuel ⁻¹		fuel ⁻¹					fuel ⁻¹			
PM _{2.5}	61.7±24.5	3.4±1.4	33.4±25.6	2.5±1.9	3.9	2.4	18.0	-	-	1.5	1.0
EC	10.7±3.6	0.6±0.2	2.4±1.6	0.2±0.1	3.0	0.6	12.2	11.2-20.0	1.2-1.7	-	-
POA	41.7±9.8	2.3±0.6	25.0±0.3	1.9±0.1	0.4	0.6	5.2	24.5-19.7	0.4-1.4	-	-
OC/EC	3.2		8.7		0.1	0.8	0.4	0.2-1.8		-	-
PAHs(×10 ⁶)	20.4±2.1	1.1±0.1	13.2±4.1	1.0±0.3	-	-	-	-	-	-	-

536
537

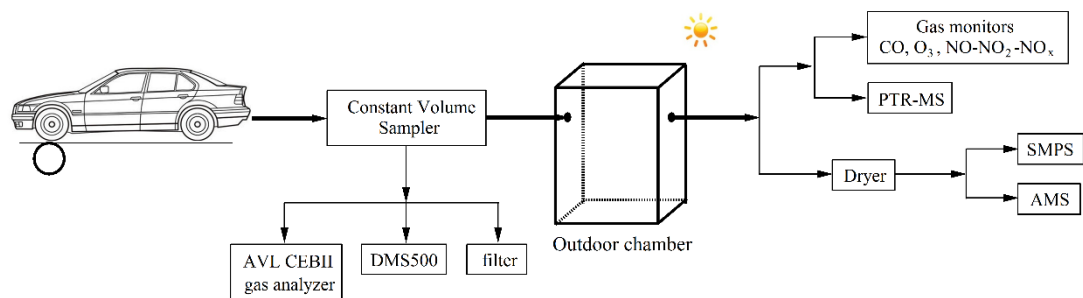
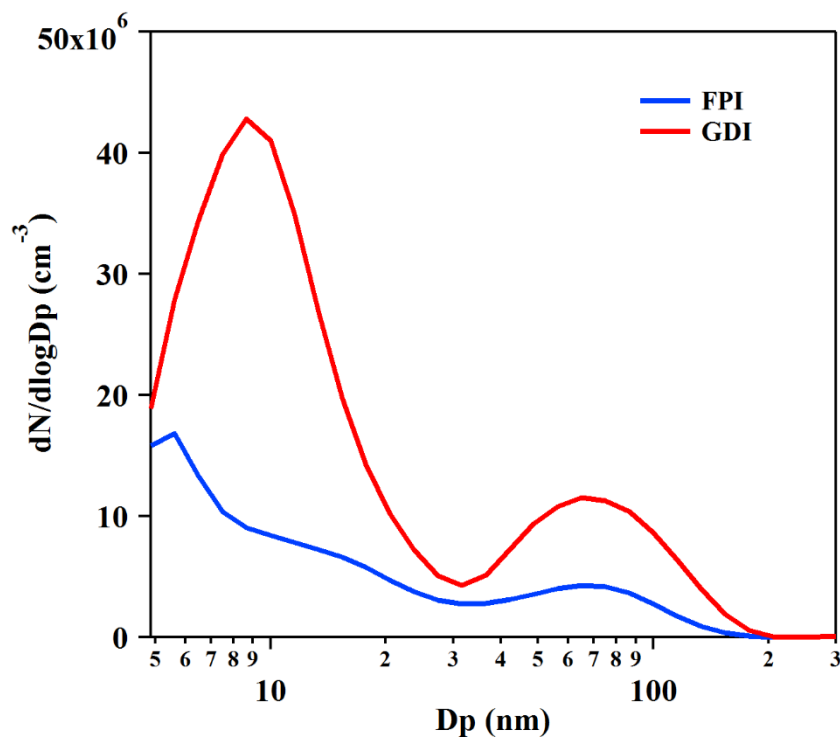


Figure 1. Schematic diagram of the outdoor chamber set up for the experiments.



541
 542 Figure 2. Number size distributions of primary PM emitted from the GDI (red line) and PFI (blue line) gasoline
 543 vehicles. The results are average of particle number emissions from vehicles during a whole BJC, measured by
 544 DMS500 in the CVS system. The particles were heated to 150°C in the DMS500.
 545

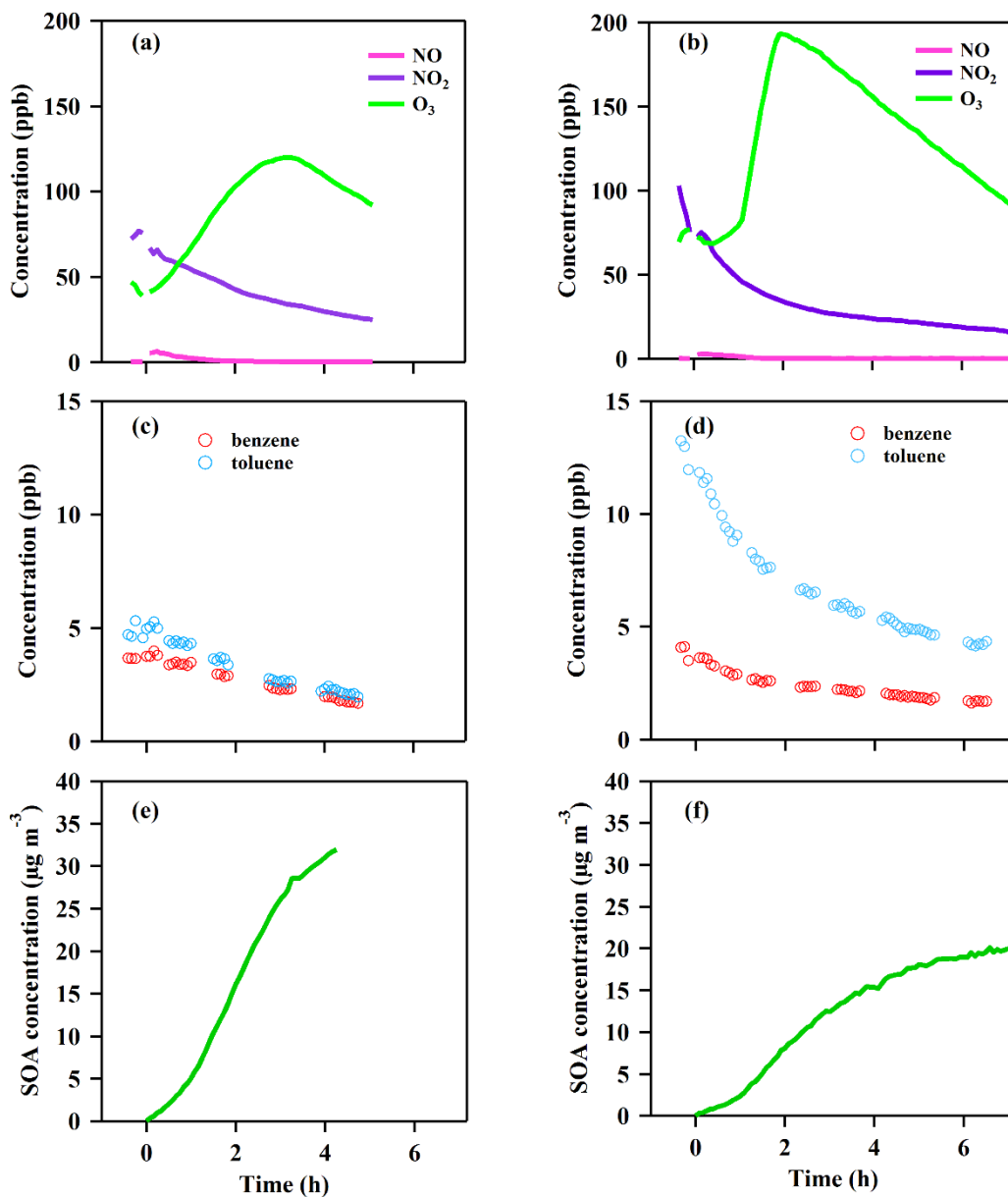
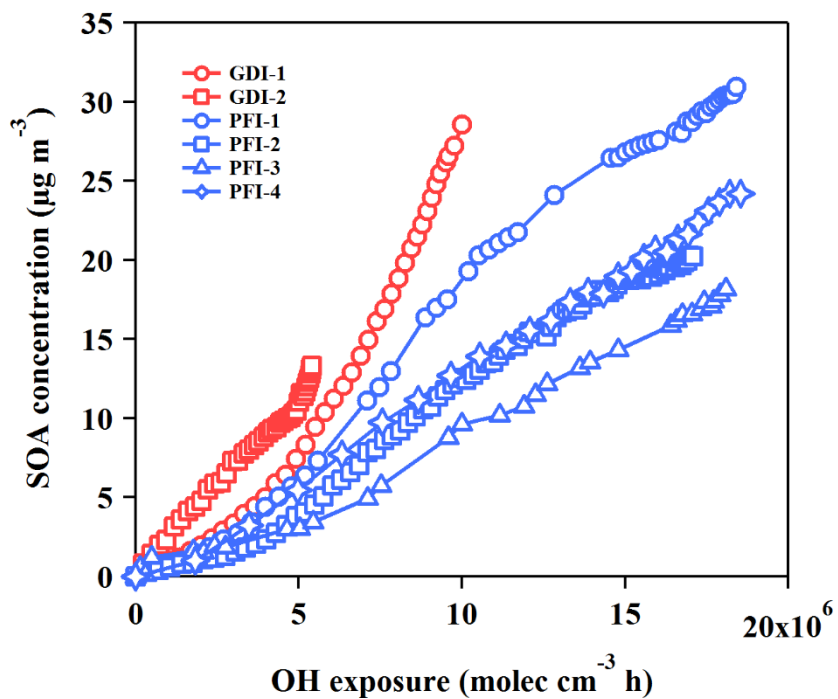


Figure 3. Time series of the gases and particle evolutions over the photochemical age in the chamber experiments from the GDI vehicle exhaust (a, c, e) and PFI vehicle exhaust (b, d, f). (a, b): NO, NO₂ and O₃ concentration; (c, d): benzene and toluene concentration; (e, f): corrected SOA concentration.



551
 552 Figure 4. SOA productions from the GDI vehicle exhaust (red markers) and the PFI vehicle exhaust (blue markers)
 553 as functions of OH exposure in the chamber experiments.
 554

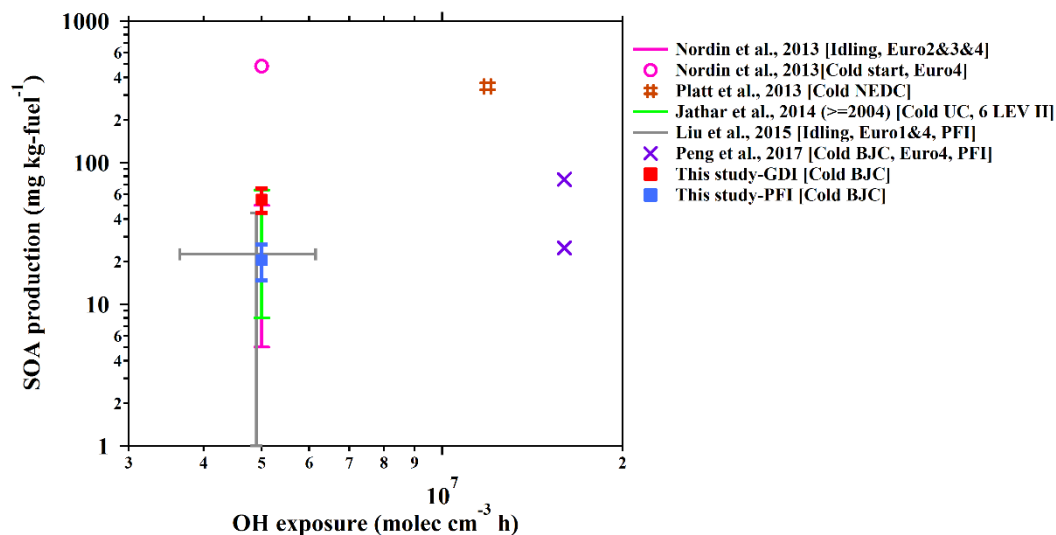
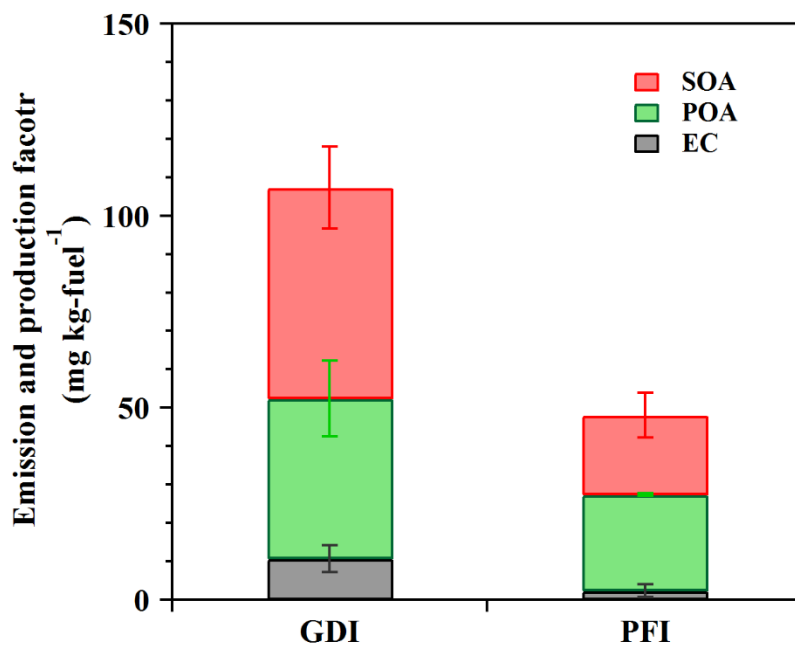


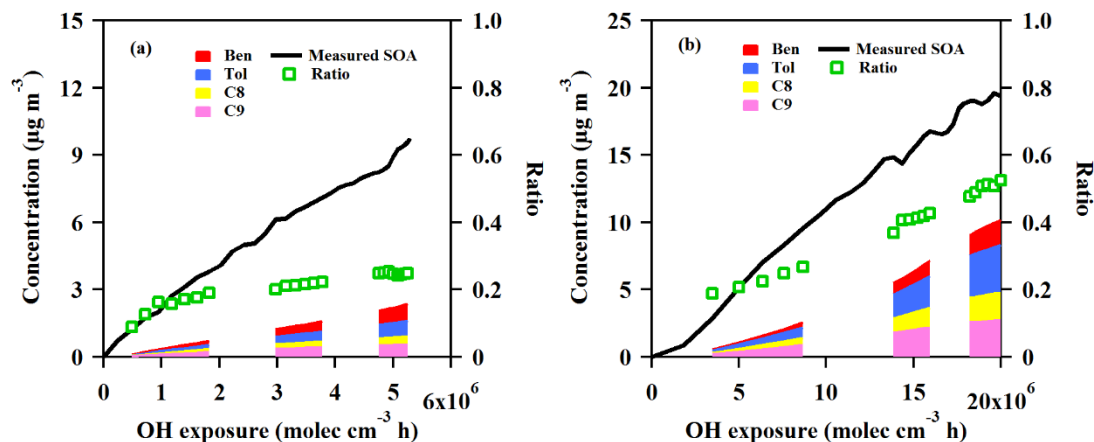
Figure 5. Fuel-based SOA production from gasoline vehicle exhaust as a function of OH exposure in the chamber simulations. The SOA production data are from published studies of chamber simulation of gasoline vehicle exhaust. From the study of Jathar et al. (2014), the SOA production of vehicles manufactured in 2004 or later (LEV II) is selected, which is a model year that is more close to those of the vehicles in this study. The error bars of previous results indicate the range of OH exposure (x axis) and SOA production (y axis) in their simulations. The driving cycles and vehicle information are also noted in the legend of each study.



563

564 Figure 6 EC and POA EFs as well as corrected SOA production factors from the GDI and PFI vehicle exhausts in
 565 this study (OH exposure = 5×10^6 molecular cm⁻³ h).

566



567

568 Figure 7. Measured and predicted SOA concentration as a function of OH exposure from GDI vehicle exhaust (a)
 569 and PFI vehicle exhaust (b) in the chamber experiments. The black line is the measured SOA concentration with
 570 wall-loss and particle dilution correction during the experiment. The red, blue, yellow and pink areas are predicted
 571 SOA concentration estimated from benzene, toluene, C8 benzene and C9 benzene, respectively. The green markers
 572 are the ratios of the predicted SOA to the measured SOA.

573

Supplementary information

Comparison of primary aerosol emission and secondary aerosol formation from gasoline direct injection and port fuel injection vehicles

Zhuofei Du¹, Min Hu^{1, 3*}, Jianfei Peng^{1†}, Wenbin Zhang², Jing Zheng¹, Fangting Gu¹, Yanhong Qin¹, Yudong Yang¹, Mengren Li¹, Yusheng Wu¹, Min Shao¹, Shijin Shuai²

1. State Key Joint Laboratory of Environmental Simulation and Pollution Control, College of Environmental Sciences and Engineering, Peking University, Beijing 100871, China

2. State Key Laboratory of Automotive Safety and Energy, Department of Automotive Engineering, Tsinghua University, Beijing 100084, China

3. Beijing Innovation Center for Engineering Sciences and Advanced Technology, Peking University, Beijing 100871, China

[†] Now at Department of Atmospheric Sciences, Texas A&M University, College Station, TX 77843, US

*Corresponding author: Min Hu, minhu@pku.edu.cn

Data correction

Wall-loss correction as well as particle and gas dilution corrections were considered in this study. The details of wall-loss correction are introduced by Du et al. (2017). The real-time instruments sampled from the chamber during the whole photo-oxidation experiment, and zero air was added to maintain a constant pressure inside the chamber. This led to particle dilution that the sampled particles would not be included in the subsequent measurement, and gas dilution that the sampled gas would not participate in the subsequent photo-oxidation reaction and SOA formation. The particle dilution corrected mass concentration $C_{corr,n+1}$ could be calculated as:

$$C_{corr,n+1} = C_{n+1} + \sum_{i=1}^n (k_{wall} \times C_i) + \sum_{i=1}^n (k_{dilu,i} \times C_i) \quad (1)$$

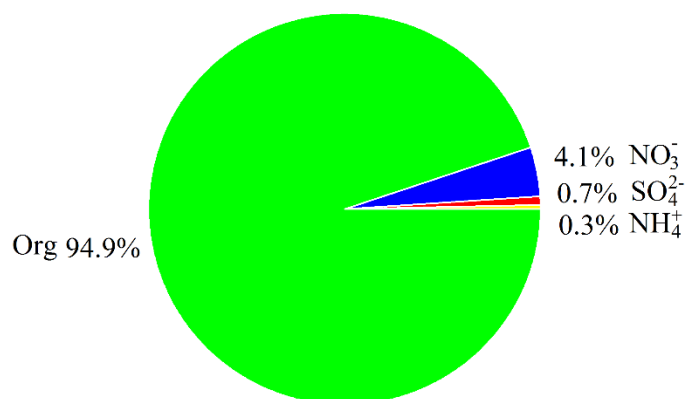
where C_{n+1} was the measured particle mass concentration at time n+1, k_{wall} was the wall loss decay constant and $k_{dilu,i}$ was dilution ratio at time i.

Then the gas dilution was taken into consideration. The final particle mass concentration $C_{final,n+1}$ could be calculated as:

$$C_{final,n+1} = C_{corr,n+1} - C_1 + \sum_{i=1}^n (\sum_{j=1}^{n+1} k_{dilu,i}) \times (C_{corr,n+1} - C_{corr,n}) \quad (2)$$

References

Du, Z., Hu, M., Peng, J., Guo, S., Zheng, R., Zheng, J., Shang, D., Qin, Y., Niu, H., Li, M., Yang, Y., Lu, S., Wu, Y., Shao, M., and Shuai, S.: Potential of secondary aerosol formation from Chinese gasoline engine exhaust, Journal of environmental sciences, in press.



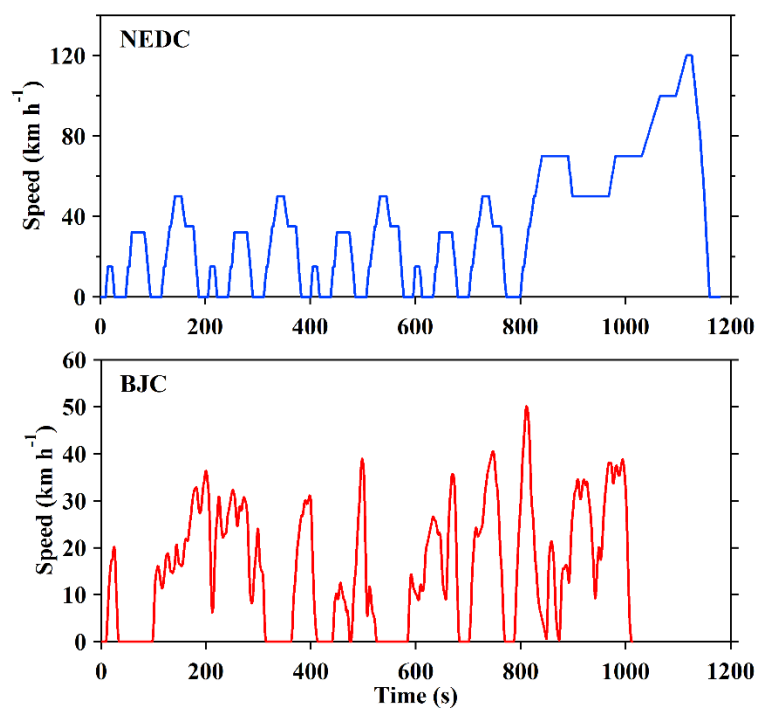
41

42 Figure S1. Chemical composition of secondary aerosol formed in the chamber experiment

43 (Experiment GDI-1).

44

45



46

47 **Figure S2. Speed profiles of NEDC and BJC driving cycle.**

48

49 Table S1 Details of the fuel used in the experiments.

Specifications	Fuel
Density (g mL ⁻¹)	0.7
Rvp (kPa)	55.4
Aromatics (% v/v)	36.7
Olefin (% v/v)	15.4
Ethanol (% v/v)	0.01
Oxygen (% m/m)	0.02
Mn (mg kg ⁻¹)	< 0.1
Sulfur (mg kg ⁻¹)	6
T10 (°C)	55.4
T50 (°C)	109.9
T90 (°C)	164.3
Fbp (°C)	194.4

50

51

Table S2 The EFs of Particulate-phase PAHs from GDI and PFI vehicles.

Compound	Emission factor (ng kg-fuel ⁻¹)	
	GDI	PFI
Napthalene	0.025	<0.0001
1-Methylnaphthalene	<0.0001	<0.0001
2-Methylnaphthalene	0.012	0.004
2,6-Dimethylnaphthalene	0.006	0.003
Acenaphthylene	0.012	0.009
Acenaphthene	<0.0001	0.015
Fluorene	0.003	0.105
Methyl-fluorene	0.083	0.105
Dibenzofuran	0.006	0.039
Retene	0.009	0.011
9-Methylanthracene	<0.0001	0.013
Phenanthrene	0.244	0.069
Anthracene	0.048	0.018
Fluoranthene	0.201	0.034
Pyrene	0.246	0.029
Methyl-fluoranthene	0.004	0.007
Benzo[a]anthracene	0.006	0.036
Chrysene	0.020	0.065
Methyl-chrysene	<0.0001	0.007
Benzo[b]fluoranthene	0.034	0.147
Benzo[k]fluoranthene	0.041	0.129
Benzo[e]pyrene	0.028	0.051
Benzo[a]pyrene	0.012	0.041
Benzo[ghi]fluoranthene	0.095	0.027
Cyclopenta[cd]pyrene	<0.0001	0.032
Dibenzo[a,h]anthracene	<0.0001	<0.0001

Picene	<0.0001	<0.0001
Perylene	0.009	<0.0001
Benzo[ghi]perylene	<0.0001	<0.0001
Indeno[1,2,3-cd]pyrene	<0.0001	<0.0001
Coronene	<0.0001	<0.0001
Sum PAHs	1.144	0.994